A Convex Relaxation for Model Predictive Control of a Class of Hammerstein Systems

Tyrone L. Vincent, Gongguo Tang, and Peter Weddle

***Abstract*—This letter provides conditions under which a structured optimization problem has a convex relaxation. In this optimization problem, the objective function and constraints can be expressed as a function of an optimization variable and a nonlinear function of this variable. A natural application of this optimization problem is model predictive control of a system that has linear dynamics, but for which the input is a non-invertible nonlinear function of an input signal. An example of such a problem is provided in the application of advanced battery management.**

***Index Terms*—Optimization methods, nonlinear control systems, battery management systems.**

I. Introduction

In this letter, the following optimization problem is of central interest

$$\begin{aligned} \min_x \ & b^T x + c^T g(x), \\ \text{subject to } & f(x, g(x)) \leq \mathbf{0}, \end{aligned} \tag{1}$$

where $x, b, c \in \mathbb{R}^n$, $g(x) : \mathbb{R}^n \to \mathbb{R}^n$ is a convex function, $f(x, y) : \mathbb{R}^n \times \mathbb{R}^n \to \mathbb{R}^m$ is convex in both arguments, $\mathbf{0} \in \mathbb{R}^m$ is a vector of zeros, and $\leq$ operates element-wise. A key assumption that will be applied is that $\mathsf{D}g$, the Jacobian of g with respect to its arguments, is a diagonal matrix (i.e., $g(x)$ is a Cartesian product of 1-D functions). Note that the composition $f(x, g(x))$ is not necessarily convex unless $f(x, y)$ non-decreasing in each element of y [1, p. 86].

This optimization problem is of interest for a variety of uses, but as specific motivation for further study we consider the application of model predictive control (MPC) for battery management. For this problem, the system behavior can be well captured by a linear system that has input u along with a static, convex, nonlinear transformation $g(u)$. The configuration of a static nonlinearity followed by a linear system is often called a Hammerstein system [2]. MPC for Hammerstein systems is straightforward if the nonlinearity is invertible [3], but for the configuration for this application (shown in Figure 2), the static function includes both u and $g(u)$ so the dimensions of the domain and range differ. The main restriction on our results is the requirement that $g(\cdot)$ operates element-wise.

We will develop a convex relaxation technique to transform the non-convex optimization (1) into a convex one and establish conditions that guarantee tightness of the relaxation. Convex relaxations are widely employed to obtain convex programs, which have a rich theory and admit algorithms with guaranteed convergence properties. However, the development of convex relaxations is more an art than science. The most straightforward way to convexify an optimization is replacing certain non-convex constraints by convex ones, for example, replacing binary $\{0, 1\}$ constraint using the interval $[0, 1]$ [4]. Lifting variables into higher-dimensional spaces and replacing the resulting nonconvex constraints with linear matrix inequalities is a powerful relaxation technique that finds applications in combinatorics, quadratically constrained quadratic programming, and optimizations involving low-rank matrices [5]–[8]. For polynomial optimization, a popular relaxation idea expresses a nonnegative polynomial constraint as the sum-of-squares [9]. Furthermore, ℓ_1 norm based relaxation and its generalizations such as the atomic norm finds applications in signal processing and machine learning [10]. Last but not least, one can, in principle, relax any nonconvex optimization into a convex one by focusing on the Lagrangian constructed bi-dual, though this is not guaranteed to yield the tightest relaxation [1]. The relaxation developed in this letter is a novel one and does not fall into any of the categories discussed above.

The convex relaxation is presented in Section II. Examples of relevant problems are given in Section III, including the application to MPC control of a Hammerstein system. Concluding remarks are given in Section IV.

A. Additional Notation

The symbol $\mathbf{1}$ is a vector of all ones, and

$$\text{sign}(x) = \begin{cases} 1 & x \geq 0 \\ 0 & x = 0 \\ -1 & x \leq 0, \end{cases}$$

with $\text{sign}(x)$ acting element-wise on vectors. For vector $x \in \mathbb{R}^n$, $[x]_i$ is the ith element of x. For function $L(x, y)$, $\mathsf{D}_x L$ is

Manuscript received February 27, 2019; revised May 6, 2019; accepted May 24, 2019. Date of publication May 31, 2019; date of current version June 10, 2019. This work was supported by the Office of Naval Research under Grant N00014-16-1-2780 and Grant N00014-17-1-2697. Recommended by Senior Editor F. Dabbene. *(Corresponding author: Tyrone L. Vincent.)*

T. L. Vincent and G. Tang are with the Department of Electrical Engineering, Colorado School of Mines, Golden, CO 80401 USA (e-mail: tvincent@mines.edu).

P. Weddle is with the Department of Mechanical Engineering, Colorado School of Mines, Golden, CO 80401 USA.

Digital Object Identifier 10.1109/LCSYS.2019.2920177

the Jacobian of L with respect to x. $\nabla_x L$ is the gradient of L with respect to x.

II. Main Result

The central idea for solving (1) is to introduce a new variable y that replaces $g(x)$, and add the constraint $g(x) \leq y$, resulting in the convex relaxation

$$\begin{aligned} \min_{x,y} \quad & b^T x + c^T y \\ \text{subject to} \quad & f(x,y) \leq \mathbf{0} \\ & g(x) - y \leq \mathbf{0}. \end{aligned} \tag{2}$$

Clearly, a solution for the relaxation is a solution for the original problem whenever the solution satisfies $g(x) = y$. The contributions of this letter are conditions on the problem that can be checked in order to guarantee that the constraint $g(x) \leq y$ is active at the solution.

Theorem 1: Suppose (2) satisfies Slater's condition, i.e., there exists (x, y) such that $f(x, y) < \mathbf{0}$ and $g(x) - y < \mathbf{0}$. An optimizer of (2) is an optimizer for (1) if for all feasible (x, y) at least one of the following are satisfied for $i = 1, \ldots, n$:

- $[c]_i = 0$, $[b]_i \neq 0$ and either $\operatorname{sign}(\mathsf{D}_{[y]_i} f) = \mathbf{1}$ or $\operatorname{sign}(\mathsf{D}_{[y]_i} f) = -\mathbf{1}$,
- $[b]_i \neq 0$ and $\operatorname{sign}([b]_i) \operatorname{sign}(\mathsf{D}_{[x]_i} f) \geq \mathbf{0}$,
- $[c]_i \neq 0$ and $\operatorname{sign}([c]_i) \operatorname{sign}(\mathsf{D}_{[y]_i} f) \geq \mathbf{0}$.

Proof: Consider the Lagrangian

$$L(x, y; \lambda, \mu) := b^T x + c^T y + \lambda^T f(x, y) + \mu^T (g(x) - y)$$

where the dual variables are $\lambda, \mu \geq 0$. Since Slater's condition is satisfied and the problem (2) is convex, strong duality holds and x, y is primal optimal if and only if there exists λ, μ such that the Karush-Kuhn-Tucker (KKT) conditions are satisfied [1, Sec. 5.5.3]:

$$\begin{aligned} & f(x,y) \leq \mathbf{0},\ g(x) \leq y, \\ & \lambda, \mu \geq \mathbf{0}, \\ & \nabla_x L = b + (\mathsf{D}_x f)^T \lambda + (\mathsf{D} g)^T \mu = \mathbf{0}, \\ & \nabla_y L = c + (\mathsf{D}_y f)^T \lambda - \mu = \mathbf{0}, \\ & [\lambda]_j f_j(x,y) = 0,\ j = 1, \ldots, m, \\ & [\mu]_i (g_i(x) - [y]_i) = 0,\ i = 1, \ldots, n. \end{aligned}$$

The theorem statement is true if the optimizer of (2) satisfies $g(x) = y$. A sufficient condition for $g(x) = y$ at the optimal point is the existence of $\mu > 0$, $\lambda \geq 0$ such that all the KKT conditions are satisfied. Suppose to the contrary that a point is optimal but there exists a set $\mathcal{I}$ such that $[\mu]_i = 0$ for $i \in \mathcal{I}$. For each $i \in \mathcal{I}$, we apply the following analysis depending on the condition in the theorem statement that is satisfied.

- For i satisfying Case 1: By the KKT conditions,

$$\begin{aligned} \mu &= c + (\mathsf{D}_y f)^T \lambda, \\ (\mathsf{D} g)^T \mu &= -b - (\mathsf{D}_x f)^T \lambda. \end{aligned}$$

  Since $[c]_i = 0$, $(\mathsf{D} g)^T$ is diagonal and $[\mu]_i = 0$,

$$\begin{aligned} 0 &= (\mathsf{D}_{[y]_i} f)^T \lambda, \\ 0 &= -[b]_i - (\mathsf{D}_{[x]_i} f)^T \lambda. \end{aligned}$$

  Since either $\operatorname{sign}(D_{[y]_i} f) = \mathbf{1}$ or $\operatorname{sign}(D_{[y]_i} f) = -\mathbf{1}$, the first equation implies $\lambda = 0$, however, since $[b]_i \neq 0$ this does not satisfy the second equation, leading to a contradiction.
- For i satisfying Case 2: By the KKT conditions

$$b + (\mathsf{D}_x f)^T \lambda = -(\mathsf{D} g)^T \mu.$$

  Since $[\mu]_i = 0$ and $(\mathsf{D} g)^T$ is diagonal,

$$[b]_i + (\mathsf{D}_{[x]_i} f)^T \lambda = 0.$$

  However, if $[b]_i \neq 0$ and the non-zero elements of $D_{[x]_i} f$ are the same sign as $[b]_i$, then we cannot have $\lambda \geq 0$, which is a contradiction.
- For i satisfying Case 3: By the KKT conditions,

$$[\mu]_i = [c]_i + (\mathsf{D}_{y_i} f)^T \lambda.$$

  However, since $[\mu]_i = 0$, $[c]_i \neq 0$ and the non-zero elements of $D_{[y]_i} f$ are the same sign as $[c]_i$, no solution exists with $\lambda \geq 0$, leading to a contradiction. ∎

Remark 1: If $\operatorname{sign}(D_{[y]_i} f) = \mathbf{1}$, is true for all i, then the original problem (1) is convex. However, depending on the problem and/or solver, it may still be more convenient to express the problem as (2), as the solver may not have built in methods to implement (1) directly, especially if $\operatorname{sign}(D_{[y]_i} f) = \mathbf{1}$ is true for feasible (x, y) but not everywhere.

III. Examples

A. Example 1

Consider the problem

$$\begin{aligned} \min \quad & bx + cx^2 \\ \text{subject to} \quad & x - x^2 \leq -1, \end{aligned} \tag{3}$$

with $b = c = 1$. Note that the constraint is equivalent to the non-convex constraint

$$x \in \left(-\infty, \frac{1-\sqrt{5}}{2}\right] \cup \left[\frac{1+\sqrt{5}}{2}, \infty\right).$$

Also note that the objective function is quadratic. When $b = c = 1$, the unconstrained minimum is at $x = -0.5$. With the constraint, the minimizer is $x = \frac{1-\sqrt{5}}{2}$ and the optimal (minimal) value of the optimization is $2 - \sqrt{5} \approx -0.236$. In the notation used above, $f(x, y) = x - y + 1$ and $g(x) = x^2$. Since Slater's condition apparently holds, $b = 1$ and $\mathsf{D}_x f = 1$, by Theorem 1 the following convex relaxation has the same minimizer as the original problem:

$$\begin{aligned} \min \quad & bx + cy \\ \text{subject to} \quad & x - y + 1 \leq 0 \\ & x^2 \leq y. \end{aligned} \tag{4}$$

Figure 1 illustrates the constraint set for the relaxed problem, with feasible points in grey.

Because the objective function is linear, any finite minimizer must occur with at least one constraint active. The conditions on b and $\mathsf{D}_x f$ ensure that the active constraint set includes $x^2 \leq y$. By the theorem, this conclusion holds for any $b > 0$, so the gradient of the objective function needs only point to

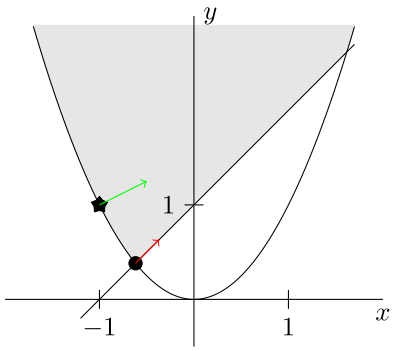

Fig. 1. Constraint set for problem 3. Feasible points are in gray. For $b = 1$ the minimizer is indicated with a circle and the gradient is in red. For $b = 2$ the minimizer is indicated with a star and the gradient is in green.

the right for the correct solution to be found. In Figure 1 the gradient at the minimizer $x = \frac{1-\sqrt{5}}{2}$, $y = \frac{3-\sqrt{5}}{2}$ is shown in red. Note that both constraints of the relaxation are active. If we change the objective function to $2x + x^2$ (i.e., $b = 2$) the minimum is at $x = -1$, and the constraint is no longer active in the original problem. In Figure 1, the gradient at the minimizer for $b = 2$, which is $x = -1$, $y = 1$, is shown in green. As is expected, for the relaxation only the constraint $x^2 \leq y$ is active.

The Lagrange bi-dual relaxation is not tight for (3). To see this, we note that standard Lagrange analysis gives the Lagrange dual optimization as

$$\underset{\lambda}{\text{maximize}} \ \frac{5\lambda^2 + \lambda + 1}{4(1-\lambda)} \ \text{subject to} \ \ 0 \leq \lambda < 1.$$

This maximization optimization is convex and has an optimal (maximal) value $-\frac{1}{4}$. Its Lagrange dual (i.e., the bi-dual) has the same optimal value, which is smaller than the optimal value of (3). Hence, the Lagrange bi-dual relaxation is not tight in this case. Note the Lagrange dual and bi-dual depend on the specific equalities and inequalities that specify the feasible region. The Frenchel dual function, defined as $f^*(z) = \sup_{x \in X} zx + (x + x^2)$ where $X := \{x : x - x^2 \leq -1\}$ is independent of the feasible region specifications. The Frenchel bi-dual function for this example corresponds to the lower convex envelope of the function defined as $x + x^2$ over X and $+\infty$ otherwise. This relaxation is apparently tight. However, for general optimization like the one shown in (1), it's usually very difficult to find the Frenchel dual and bi-dual.

Problem (3) is also a quadratically constrained quadratic program (QCQP), and the optimization (4) coincides with the convex relaxation constructed by the lifting method for QCQP. However, it should be emphasized that Theorem 1 applies for general diagonal functions $g(x)$ while the lifting method applies for outer products, so these methods diverge strongly in higher dimensions.

B. Example 2: Model Predictive Control for Battery Management

This example provides a specific illustration of model predictive control applied to a system that is linear except for a static nonlinear mapping at the input. Model predictive control is used in a variety ways in systems that include batteries. The most common applications are systems with multiple energy sources, such as micro-grids [11], hybrid vehicles [12]–[15] and hybrid power sources [15]–[17]. In these cases, constraints on the state of charge and battery voltage are the primary consideration, and the battery model is typically a relatively simple equivalent-circuit model. However, because battery aging and damage can occur even when voltage limits are respected, there have been efforts to apply MPC with more sophisticated models. An important example of this case is the control of battery charging with constraints on state of charge and temperature [18]. A related approach uses online calculation of the current required to meet overpotential constraints [19].

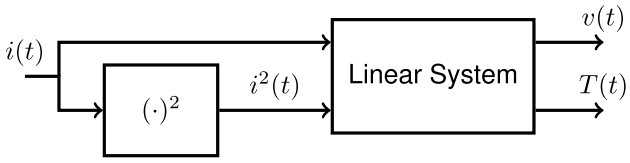

Fig. 2. Block diagram of battery model with static nonlinear transformation applied to an input.

Consider operating a battery with the applied current (i) as a controlled input (where i is positive when charging). In practice, control of current can be achieved using power electronics [20]. Two major observables that help determine safe battery operation are the voltage (v) across the terminals and the battery operating temperature (T). At a specific state of charge, for small currents, the voltage depends linearly on the current, but the temperature response is fundamentally nonlinear as it is primarily due to ohmic heating and will depend on the square of the current. This gives rise to the model structure shown in Figure 2. Further comments on the appropriateness of this model are below.

The system is controlled using model predictive control with sampling time T_s. The battery management objectives can take a variety of forms, but for this example we consider two cases. First, a fast charging application is studied where stored charge is maximized, while respecting constraints imposed on the terminal voltage and operating temperature. The second application is the complementary case: maximize the discharge rate, subject to the same constraints, say as part of a grid storage system for frequency regulation.

Collect the system outputs at sampling interval k in vector y_k, and let u_k be the current at sampling interval k. That is,

$$y_k = \begin{bmatrix} v(kT_s) \\ T(kT_s) \end{bmatrix}, \quad \text{and} \quad u_k = \begin{bmatrix} i(kT_s) \end{bmatrix}.$$

We assume that the voltage and temperature constraints are time-invariant and can be expressed as a convex constraint

$$h(v, T) \leq 0.$$

An example of such a constraint is shown in Figure 4. In this case, h is simply a linear function.

Without loss of generality, let the current time sample be $k = 0$. Collect past and future inputs and outputs over finite

windows as follows:

$$U_p = \begin{bmatrix} u_{-1} \\ u_{-2} \\ \vdots \\ u_{-n_p} \end{bmatrix}, \; U_f = \begin{bmatrix} u_0 \\ u_1 \\ \vdots \\ u_{n_f} \end{bmatrix}, \; Y_p = \begin{bmatrix} y_{-1} \\ y_{-2} \\ \vdots \\ y_{-n_p} \end{bmatrix}, \; Y_f = \begin{bmatrix} y_0 \\ y_1 \\ \vdots \\ y_{n_f} \end{bmatrix}.$$

where n_p and n_f are integers that define the past and future window sizes.

We assume that predictions of the future trajectories of voltage and temperature can be obtained using an Auto-Regressive eXogenous (ARX) structure that is linear in the future inputs, namely a function P of the form

$$Y_f = P(U_p, U_p^2, Y_p, U_f, U_f^2),$$

where $(.)^2$ is applied element-wise. In this case, past inputs and outputs along with future inputs are used to predict future outputs. This function could be obtained via system identification, or could be the result of using a model to derive an estimator and predictor.

Let H be the n_f times Cartesian product of h. Then feasible system trajectories (i.e., those for which the temperature and voltage constraints are satisfied) satisfy the composition $F = H \circ P \leq \mathbf{0}$. Since U_p, U_p^2, Y_p are known and constant at time 0, represent this composition as

$$F(U_f, U_f^2) \leq \mathbf{0}.$$

Note that since P is linear in U_f and U_f^2, and H is convex, F is convex.

A bare-bones MPC formulation for fast but safe charging ($a = -1$) or discharging ($a = 1$) would be as follows,

$$\min_{U_f} \; a\mathbf{1}^T U_f + \epsilon \mathbf{1}^T U_f^2$$
$$\text{subject to} \; \; F(U_f, U_f^2) \leq \mathbf{0}.$$

The objective function is the sum of two terms. The first is the negative of the net charge applied (for $a = -1$) or withdrawn (for $a = 1$) over a window into the future of length n_f. The MPC will seek to maximize the net charge transfer. The second is the sum of the squared currents, weighted by a small value $\epsilon > 0$. Clearly as ϵ goes to zero, the objective function measures only the charge transfer, but this second term will be useful to expand the conditions under which a relaxation provides an exact solution.

A more sophisticated application may also include a modification to ensure feasibility, for example by adding auxiliary variables to create soft constraints, or additional constraints to ensure stability. However, the formulation above is still applicable in the nominal case when these additional terms are not active.

To apply the convex reformulation discussed in this letter, an additional variable Z is defined that is the same size as U_f. This variable replaces U_f^2, and an additional constraint is added,

$$\min_{U_f, Z} \; a\mathbf{1}^T U_f + \epsilon \mathbf{1}^T Z$$
$$\text{subject to} \; \; F(U_f, Z) \leq \mathbf{0}$$
$$U_f^2 \leq Z.$$

Assuming Slater's condition holds (as is the case for the example shown in Figure 4) and using Theorem 1, the following conditions imply that the solution for the relaxation provides a minimizer for the original problem.

- if $a = 1$ the reformulation is valid if either
  - $\text{sign}(\mathsf{D}_{U_f} F) \geq \mathbf{0}$ or
  - $\text{sign}(\mathsf{D}_Z F) \geq \mathbf{0}$.
- if $a = -1$, the reformulation is valid if either
  - $\text{sign}(\mathsf{D}_{U_f} F) \leq \mathbf{0}$ or
  - $\text{sign}(\mathsf{D}_Z F) \geq \mathbf{0}$.

Remark 2: These conditions depend on the form of the predictor and constraints, but in principle can be verified a-priori. A specific example is provided below.

Remark 3: A real battery is nonlinear, both due to a nonlinear open circuit voltage and changes in the charge transfer dynamics at different states of charge. The approach outlined here could still be applied using a gain scheduled approach, so that the linear model changes with operating conditions perhaps complemented with a robust implementation, where the constraints are checked using multiple realizations of the predictor [21]–[23].

As a concrete example that demonstrates the conditions of validity for the convex relaxation, we consider a battery with a voltage dynamic model as shown in Figure 3(a). In this diagram, V_{oc} is the open circuit voltage, which is a function of the state of charge. For this simulation, the open circuit voltage will have the response shown in Figure 3(b), while the state of charge is given by

$$s(t) = \frac{100}{A} \int_{t_0}^{t} i(t)dt + s(t_0),$$

where $s(t_0)$ is the initial state of charge in percent and A is the battery capacity in amp-seconds. The battery is fully charged when $s(t) = 100\%$. The temperature dynamic response is given by the differential equation

$$\dot{T} = -\alpha(T - T_\infty) + \kappa i^2, \tag{5}$$

where α and κ are parameters. The first term in the temperature model captures convection to the environment, while the second term captures ohmic heating effects. It should be noted that the thermal model does not include Faradaic heating [24]. The more complex current dependencies introduced by Faradaic heat generation is not considered in this letter to keep the example straightforward. However, Theorem 1 would still apply to the more complex heating model which will include additional terms of the form $\gamma_1 i \sinh(\gamma_2 i)$ and $\gamma_3 i$, where γ_n are functions of the current battery state.

For this application temperature and voltage are assumed to be measured. The predictor (i.e., the function $F(\cdot)$) is the sum of two components, the value of the outputs at the current time, plus the predicted change in these values over the future time window.

To calculate the predicted change, the voltage dynamics are linearized by replacing the open circuit voltage V_{oc} with an equivalent capacitor C_{oc}. At a particular state of charge, the value of this capacitor should be $C_{oc} = \frac{A}{100} \frac{1}{\frac{dV_{oc}}{ds}}$. The state

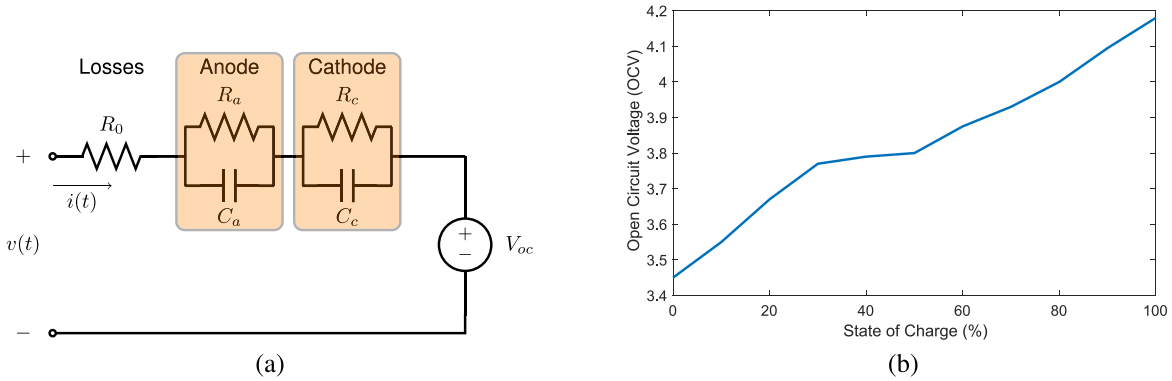

(a) (b)

Fig. 3. (a) Battery equivalent circuit model use for simulations. (b) Open circuit voltage for simulated battery.

space representation of this model is

$$\dot{x}(t) = Ax(t) + B\begin{bmatrix} u(t) \\ u^2(t) \end{bmatrix}$$
$$y(t) = Cx(t) + D\begin{bmatrix} u(t) \\ u^2(t) \end{bmatrix}, \tag{6}$$

where

$$A = \begin{bmatrix} -\frac{1}{R_a C_a} & 0 & 0 & 0 \\ 0 & -\frac{1}{R_c C_c} & 0 & 0 \\ 0 & 0 & 0 & 0 \\ 0 & 0 & 0 & -\alpha \end{bmatrix}, \; B = \begin{bmatrix} \frac{1}{C_a} & 0 \\ \frac{1}{C_c} & 0 \\ \frac{1}{C_{oc}} & 0 \\ 0 & \kappa \end{bmatrix}$$
$$C = \begin{bmatrix} 1 & 1 & 1 & 0 \\ 0 & 0 & 0 & 1 \end{bmatrix}, \; D = \begin{bmatrix} R_0 & 0 \\ 0 & 0 \end{bmatrix}.$$

For ease of calculation, the model (6) is converted to discrete time using a zero order hold equivalent.

$$\hat{x}_{k+1} = \Phi\hat{x}_k + \Gamma\begin{bmatrix} u_k \\ u_k^2 \end{bmatrix}$$
$$y_k = C\hat{x}_k + D\begin{bmatrix} u_k \\ u_k^2 \end{bmatrix}, \tag{7}$$

where

$$\Phi = \exp(A\Delta t), \quad \Gamma = \int_0^{T_s} \exp(A\eta)B \; d\eta.$$

Since predictions of the future trajectories are taken relative to the current output, these can be made based on input variations, rather than the absolute input. This alleviates the need to keep track of the current operating point. Specifically, let be δ the first difference operator (i.e., $\delta u_k = u_k - u_{k-1}$ and $\delta u_k^2 = u_k^2 - u_{k-1}^2$). If y_k is the response of system (7) to u_k, then δy_k can be calculated as

$$\delta y_k = C\Phi^k x_0 + D\begin{bmatrix} \delta u_k \\ \delta u_k^2 \end{bmatrix} + \sum_{\ell=0}^{k-1} C\Phi^{k-\ell} B\begin{bmatrix} \delta u_k \\ \delta u_k^2 \end{bmatrix}, \tag{8}$$

where x_0 is the state of (8) at time 0 in response to the first difference of the input. Given a measurement of the output at the current time ($k = 0$), predictions of the future trajectories can be calculated as

$$\hat{y}_k = y_0 + \sum_{\ell=1}^{k} \delta y_\ell. \tag{9}$$

where y_0 is the current measurement. This calculation requires x_0, the state of the system with first difference input and output. To obtain x_0, any estimation method may be used (e.g., Observer, Kalman Filter, Moving Horizon Estimation (MHE), etc.). The composition of (8), (9), and the estimator (with appropriate vectorization) gives a predictor function F that is linear in u_k and u_k^2.

For this demonstration, the constraint set is the intersection of the constraints

$$\begin{aligned} v_k + \beta(T_k - 25) &\leq 4.5 \\ v_k - \beta(T_k - 25) &\geq 3.2 \\ v_k &\leq 4.15 \\ v_k &\geq 3.6. \end{aligned} \tag{10}$$

The constraint with $\beta = 0.1$ is illustrated in Figure 4(a). In addition to a typical constraint on the maximum and minimum terminal voltage, a more restrictive constraint is applied when the temperature is elevated above a reference temperature. These constraints are linear, and thus so is the constraint function h, and the feasibility function F.

In order for the controller to operate in both charging and discharging model, the condition $\text{sign}(\mathsf{D}_Z F) \geq 0$ needs to be satisfied. From (8), (9) and (10), $\mathsf{D}_Z F$ can be easily calculated as

$$\mathsf{D}_Z F = \begin{bmatrix} \tilde{C}_2 B_2 & 0 & 0 & 0 \\ \tilde{C}_2 \Phi B_2 & \tilde{C}_2 B_2 & 0 & 0 \\ \vdots & \vdots & \ddots & \vdots \\ \tilde{C}_2 \Phi^{n_f - 1} B_2 & \cdots & \cdots & \cdots \end{bmatrix},$$

where

$$\tilde{C}_2 = \begin{bmatrix} \beta & \beta & 0 & 0 \end{bmatrix}^T C_2,$$

C_2 is the second row of C and B_2 is the second column of B. In fact, the matrix contains elements of the impulse response from the current squared to the temperature scaled by β. Since the temperature dynamics are first order with positive DC gain, $\text{sign}(\mathsf{D}_Z Z) \geq \mathbf{0}$ will occur as long as $\beta > 0$. Note that since $\text{sign}(\mathsf{D}_Z Z) \geq \mathbf{0}$ is true, the relaxation is exact for *any* form of voltage dynamics.

Figure 4 shows a simulation implementing the MPC controller on a sample battery. The initial state of charge is 25%. The values of the parameters used in this simulation are shown in Table I. R_0, R_a, R_c, C_a, and C_c are taken from estimates at 50% state of charge reported in [25]. The MHE is used as the estimator with a window size n_p, quadratic cost on

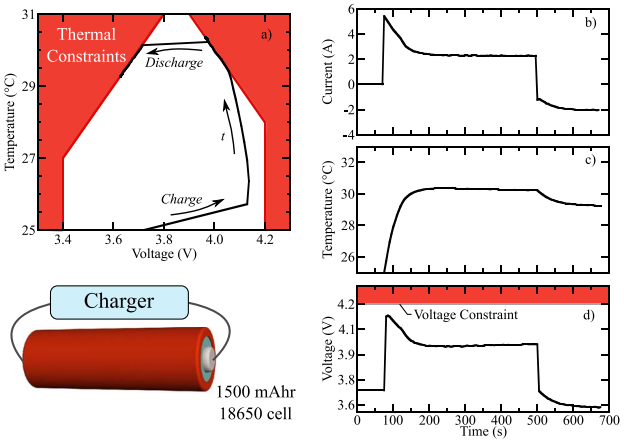

Fig. 4. Results for MPC control of battery charging and discharging. Charging is maximized subject to constraints until 500 s, then discharging is maximized.

TABLE I
PARAMETERS FOR BATTERY SIMULATION

Element	Value	Element	Value
R_0	0.06 Ω	β	.1
R_a	0.025 Ω	ϵ	1e-3
R_c	0.0086 Ω	σ	.001 mV
C_a	1181 F	Q	I
C_c	530 F	R	.1
C_{oc}	5400 F	T_s	5 s
α	0.005	n_p	15
κ	0.005	n_f	15
T_∞	25 °C	A	5400 As

disturbance and noise with weighting Q and R respectively, and no arrival cost term (see, e.g., [26]). The MPC controller starts at 75s, with $a = -1$, so that charging is maximized. At 500 s, the parameter a is changed to $a = 1$, so that discharging is maximized. For the linearized model used in the estimator C_{oc} is fixed at the value shown in Table I. By adding a state of charge estimator, this parameter could be adapted, but since it is associated with slower dynamics the controller is naturally robust to its value. Pseudo-random noise with standard deviation 0.001 V is added to the voltage measurements. Note that the controller is able to successfully meet the desired temperature/voltage constraints, and it can be verified that the constraint $U_f^2 \leq Z$ is active at every sample time.

IV. CONCLUSION

This letter provided a new convex relaxation for an optimization problem relevant to MPC for a class of Hammerstein systems for which the nonlinearity is non-invertible. The conditions for tightness of the relaxation depend on the system dynamics and can be easily checked.

ACKNOWLEDGMENT

The authors thank Dr. Robert Kee for assistance in the development of this letter.

REFERENCES

[1] S. P. Boyd and L. Vandenberghe, *Convex Optimization*. Cambridge, U.K.: Cambridge Univ. Press, 2004.
[2] I. W. Hunter and M. J. Korenberg, "The identification of nonlinear biological systems: Wiener and Hammerstein cascade models," *Biol. Cybern.*, vol. 55, nos. 2–3, pp. 135–144, 1986.
[3] K. H. Chan and J. Bao, "Model predictive control of Hammerstein systems with multivariable nonlinearities," *Ind. Eng. Chem. Res.*, vol. 46, no. 1, pp. 168–180, 2007.
[4] P. Raghavan and C. D. Tompson, "Randomized rounding: A technique for provably good algorithms and algorithmic proofs," *Combinatorica*, vol. 7, no. 4, pp. 365–374, 1987.
[5] M. X. Goemans and D. P. Williamson, "Improved approximation algorithms for maximum cut and satisfiability problems using semidefinite programming," *J. ACM*, vol. 42, no. 6, pp. 1115–1145, 1995.
[6] Z.-Q. Luo, W.-K. Ma, A. M.-C. So, Y. Ye, and S. Zhang, "Semidefinite relaxation of quadratic optimization problems," *IEEE Signal Process. Mag.*, vol. 27, no. 3, pp. 20–34, May 2010.
[7] E. J. Candes, Y. C. Eldar, T. Strohmer, and V. Voroninski, "Phase retrieval via matrix completion," *SIAM Rev.*, vol. 57, no. 2, pp. 225–251, 2015.
[8] G. Tang and B. Recht, "Convex blind deconvolution with random masks," in *Computational Optical Sensing and Imaging*, Opt. Soc. America, 2014, p. CW4C–1.
[9] L. J. Bernard, *Moments, Positive Polynomials and Their Applications*, vol. 1. Singapore: World Sci., 2009.
[10] G. Tang, B. N. Bhaskar, P. Shah, and B. Recht, "Compressed sensing off the grid," *IEEE Trans. Inf. Theory*, vol. 59, no. 11, pp. 7465–7490, Nov. 2013.
[11] A. Hooshmand, M. H. Poursaeidi, J. Mohammadpour, H. A. Malki, and K. Grigoriads, "Stochastic model predictive control method for microgrid management," in *Proc. IEEE PES Innov. Smart Grid Technol. (ISGT)*, Washington, DC, USA, 2012, pp. 1–7.
[12] S. J. Moura, J. L. Stein, and H. K. Fathy, "Battery-health conscious power management in plug-in hybrid electric vehicles via electrochemical modeling and stochastic control," *IEEE Trans. Control Syst. Technol.*, vol. 21, no. 3, pp. 679–694, May 2013.
[13] J. P. Torreglosa, P. García, L. M. Fernández, and F. Jurado, "Predictive control for the energy management of a fuel-cell–battery–supercapacitor tramway," *IEEE Trans Ind. Informat.*, vol. 10, no. 1, pp. 276–285, Feb. 2014.
[14] G. Ripaccioli, D. Bernardini, S. Di Cairano, A. Bemporad, and I. V. Kolmanovsky, " A stochastic model predictive control approach for series hybrid electric vehicle power management," in *Proc. Amer. Control Conf. (ACC)*, Baltimore, MD, USA, 2010, pp. 5844–5849.
[15] L. Valverde, C. Bordons, and F. Rosa, "Power management using model predictive control in a hydrogen-based microgrid," in *Proc. IEEE 38th Annu. Conf. Ind. Electron. Soc. (IECON)*, Montreal, QC, Canada, 2012, pp. 5669–5676.
[16] R. T. B. Amin, A. S. Rohman, C. J. Dronkers, R. Ortega, and A. Sasongko, "Energy management of fuel cell/battery/supercapacitor hybrid power sources using model predictive control," *IEEE Trans. Ind. Informat.*, vol. 10, no. 4, pp. 1992–2002, Nov. 2014.
[17] A. Vahidi, A. Stefanopoulou, and H. Peng, "Current management in a hybrid fuel cell power system: A model-predictive control approach," *IEEE Trans. Control Syst. Technol.*, vol. 14, no. 6, pp. 1047–1057, Nov. 2006.
[18] J. Yan, G. Xu, H. Qian, and Y. Xu, "Battery fast charging strategy based on model predictive control," in *Proc. IEEE 72nd Veh. Technol. Conf. Fall (VTC-Fall)*, Ottawa, ON, Canada, 2010, pp. 1–8.
[19] K. A. Smith, C. D. Rahn, and C.-Y. Wang, "Model-based electrochemical estimation and constraint management for pulse operation of lithium ion batteries," *IEEE Trans. Control Syst. Technol.*, vol. 18, no. 3, pp. 654–663, May 2010.
[20] M. Bragard, N. Soltau, S. Thomas, and R. W. De Doncker, "The balance of renewable sources and user demands in grids: Power electronics for modular battery energy storage systems," *IEEE Trans. Power Electron.*, vol. 25, no. 12, pp. 3049–3056, Dec. 2010.
[21] A. Bemporad and M. Morari, "Robust model predictive control: A survey," in *Robustness in Identification and Control* (Lecture Notes in Control and Information Sciences), vol. 245, A. Garulli and A. Tesi, Eds. London, U.K.: Springer, 1999, pp. 207–226.
[22] H. Sartipizadeh and T. L. Vincent, "A new robust MPC using an approximate convex hull," *Automatica*, vol. 92, pp. 115–122, Jun. 2018.
[23] G. C. Calafiore and M. C. Campi, "The scenario approach to robust control design," *IEEE Trans. Autom. Control*, vol. 51, no. 5, pp. 742–753, May 2006.
[24] M. Guo, G. Sikha, and R. E. White, "Single-particle model for a lithium-ion cell: Thermal behavior," *J. Electrochem. Soc.*, vol. 158, no. 2, pp. A122–A132, 2011.
[25] L. Zhang, H. Peng, Z. Ning, Z. Mu, and C. Sun, "Comparative research on RC equivalent circuit models for lithium-ion batteries of electric vehicles," *Appl. Sci.*, vol. 7, no. 10, p. 1002, 2017.
[26] D. G. Robertson, J. H. Lee, and J. B. Rawlings, "A moving horizon-based approach for least-squares estimation," *AIChE J.*, vol. 42, no. 8, pp. 2209–2224, 1996.